



Contents lists available at ScienceDirect

Bioresource Technology

journal homepage: www.elsevier.com/locate/biortech



Abundant and rare microbial sub-communities in anammox granules present contrasting assemblage patterns and metabolic functions in response to inorganic carbon stresses

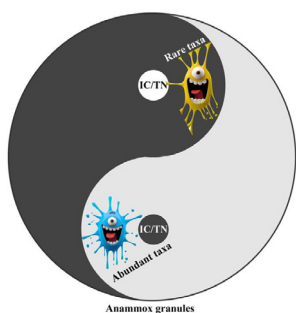


Duntao Shu^a, Baogang Zhang^a, Yanling He^b, Gehong Wei^{a,*}

^a State Key Laboratory of Crop Stress Biology in Arid Areas, College of Life Sciences, Northwest A&F University, Yangling, Shaanxi 712100, China

^b School of Human Settlements & Civil Engineering, Xi'an Jiaotong University, Shaanxi 710049, China

GRAPHICAL ABSTRACT



ARTICLE INFO

Keywords:

Rare sub-community
IC/TN ratio
Anammox
Community assembly
Functional traits

ABSTRACT

Nitrogen-transforming microorganisms play pivotal roles for the microbial nitrogen-cycling network in the anammox granular system. However, little is known about the effects of inorganic carbon (IC) stresses on the assemblage patterns and functional profiles of abundant and rare taxa. Herein, the community assemblage and functional traits of abundant and rare sub-communities were investigated. Results revealed that insufficient IC had adverse influences on the process performance, while anammox activity could be recovered by IC addition. Co-occurrence network analysis indicated that abundant and rare sub-communities present divergent co-occurrence patterns. Additionally, environmental filtering had different influences on the ecological adaptability of bacterial sub-communities. Furthermore, qPCR results illustrated that $\text{NH}_4^+\text{-N}$ and $\text{NO}_2^-\text{-N}$ consumption were regulated by abundant sub-community, while their accumulation was mediated by rare sub-community. Collectively, these findings suggest that abundant and rare sub-communities present contrasting assemblage patterns and metabolic pathways, and functional profiles dominated selection of bacterial sub-communities under IC stresses.

1. Introduction

In the last few decades, nutrient reduction and nutrient control have become increasingly pressing important issues for wastewater

treatment plants (WWTPs) (Lettinga, 2014). Biological nitrogen removal processes in industrial and municipal WWTPs are undergoing tremendous changes motivated by the strict effluent regulations that are being implemented across the world (Hendriks and Langeveld,

* Corresponding author.

E-mail address: weige hong@nwsuaf.edu.cn (G. Wei).

<https://doi.org/10.1016/j.biortech.2018.06.022>

Received 18 April 2018; Received in revised form 4 June 2018; Accepted 8 June 2018

Available online 09 June 2018

0960-8524/ © 2018 Elsevier Ltd. All rights reserved.

2017). Anaerobic ammonia oxidation (Anammox), which has emerged as an innovative, energy efficient nitrogen removal processes, is successfully applied for ammonium-rich wastewater treatment with ~100 full scale installations (Kartal et al., 2013; Lackner et al., 2014). The cosmopolitan application of anammox related technologies provides more sustainable solutions to energy neutrality and nutrient recovery of WWTPs. Given the sensitivity of anammox bacteria, environmental parameters have been regarded to be the limiting factors for the mainstream application of anammox processes.

Inorganic carbon (IC), an assimilation carbon source for chemoautotrophic bacteria, plays a key role in maintaining the stability of the anammox system. Previous literatures have reported that long-term addition of IC significantly enhanced the nitrogen removal efficiency in a single anammox system (Jin et al., 2014; Kimura et al., 2011). In the nitrification-anammox process, IC has been shown to have a remarkable influence on the nitrogen-transforming microorganisms (Ma et al., 2015). In the completely autotrophic nitrogen removal over nitrite (CANON) processes, results demonstrated that *Candidatus Brocadia* was found to survive under the low IC concentrations and the influent IC/N should be set between 1.5 and 2.0 in this CANON process (Yue et al., 2018; Zhang et al., 2016). Furthermore, recent studies (Daguerre Martini et al., 2018; Zhang et al., 2018) have revealed that IC concentrations not only have positive correlations with N₂O emissions, but can also impact the resilience and resistance of anammox systems. In engineering applications, the IC/N ratios were ranged from 0.1:1 to 4:1; higher IC/N ratios (> 1.5:1) are necessary to avoid the decrease in nitrogen removal efficiency caused by an IC deficit (Ma et al., 2015). These recent studies, and others, provide insights into the effect of IC on the nitrogen removal, anammox growth, and N₂O emission, et. al. However, the influence of IC stresses on the assemblage patterns and metabolic pathways of keystone microorganisms in anammox system remains elusive, especially for those functional genera are rare but environmentally important. Therefore, it is crucial to get a clear understanding of the underlying microbial mechanism of anammox system in response to IC stresses.

Nitrogen-transforming microorganisms play pivotal roles in the microbial nitrogen-cycling network for anammox related processes. Frequently abundant or transiently abundant microorganisms comprise the core microbial community and make great contribution to nitrogen removal and carbon turnover in WWTPs (Saunders et al., 2016). Rare taxa, the low abundance microbial population, have been termed the “rare biosphere” or “rare sub-community” (Shade and Gilbert, 2015). The increasing availability and cost-efficiency of next generation sequencing technologies have led to an explosion of details about microbial communities, and their assemblage patterns, and has provided a framework for the investigation of rare sub-community. Previous literature indicates that rare sub-community contribute to patterns of microbial diversity and may perform distinct ecosystem functions. For example, some of the rare taxa present are more active than the abundant taxa (Jia et al., 2018), and rare taxa contribute substantially to protein synthesis in WWTPs (Lawson et al., 2015). In addition, the ecological functions of rare sub-community may be beneficial to environmental resistance and resilience to ecological systems (Ziegler et al., 2018). Nevertheless, studies assessing the microbial assemblage patterns of abundant and rare sub-communities in anammox system remains scarce. Only two studies have been performed, one in an activated sludge reactor (Kim et al., 2013) and the other in a simultaneous anammox and denitrification (SAD) system (Shu et al., 2018), and these results indicated that abundant and rare sub-communities exhibited contrasting assemblage patterns in terms of community structure and microbial co-occurrence networks. However, the correlations among above microbial sub-communities, nitrogen transforming pathways, and functional profiles remain poorly understood. Therefore, whether abundant taxa present divergent community assemblage patterns and different underlying functional traits compared with rare microorganisms in the anammox granular reactor remain unclear.

It is thus essential to obtain a clear understanding of the assemblage patterns of microbial sub-community and the links to the corresponding functional traits, to benefit the functional stability and facilitate the engineering of new functions of anammox system under abiotic stresses as well. Therefore, the present study intends to address the following objectives: (1) Do abundant and rare sub-communities exhibit contrasting assemblage patterns and functional traits under different IC/TN ratio stresses? If so, (2) What are the co-occurrence of abundant and rare taxa on the level of taxonomy and metabolic function? And what are the dominant drivers that affect the discrepancy of these patterns? (3) Which functional genera of bacterial sub-communities are the key regulators for the nitrogen transforming pathway?

2. Materials and methods

2.1. Anammox seeding biomass and reactor operation strategy

An expanded granular sludge blanket (EGSB) with working volume of 2.0 L (Height: 70 cm; Diameter: 6 cm) was adopted as the anammox granular reactor in the present study. Initially, 200 mL anammox biomass (2.85 g/L) was collected from a laboratory-scale sequencing batch reactor (SBR) in previous study and 600 mL denitrification sludge (7.33 g/L) was taken from landfill leachate treatment system (Jiang Cungou village, Xi'an, Shaanxi, China) as seeding sludge for the EGSB reactor. Prior to the present experiment, this anammox granular system has been running for over four years under mesophilic condition (32 ± 2 °C) with hydraulic residence time (HRT), influent NH₄⁺-N, and NO₂⁻-N concentrations of 6 h, 97.75 ± 2.8 mg-N/L and 119.64 ± 1.8 mg-N/L mg/L, respectively. The long-term removal efficiencies for NH₄⁺-N and NO₂⁻-N were 92.65 ± 0.41 and 97.14 ± 0.11%, respectively. Based on the clone library, “*Ca. Brocadia sinica*” and “*Ca. Brocadia Jettenia*” were the dominant anammox bacteria in the EGSB system.

To explore the assemblage patterns and functional traits of abundant and rare microbial sub-communities under IC stresses, the nearly 200 days of the operational period for the whole experiment was divided into nine distinct phases (Phase I-Phase IX). Phase I was set as the controlled phase without any changes of operational parameters from the previous study. In Phase II-Phase IX, distinct KHCO₃ was fed to yield an IC to TN (total nitrogen) ratio of 0–1.87. For these eight phases, HRT was controlled at 12 h. In addition, trace element solution and mineral medium containing 81.88 ± 1.19 mg/L NH₄⁺-N and 91.03 ± 1.08 mg/L NO₂⁻-N were added into the reactor automatically by peristaltic pump (BT300-2J, LongerPump, China).

2.2. DNA extraction, PCR amplification, and Illumina MiSeq sequencing

For sludge sampling, anammox biomass was collected from the EGSB reactor at the end of each phase. The collection procedure was repeated three times for each specimen. Genomic DNA from each sample (2.0 mL) was extracted using the FastDNA[®] SPIN Kit for Soil (Mp Biomedicals, Illkirch, France) according to the manufacturer's protocols. The triplicate DNA samples extracted for each phase were pooled to generate one homogenized single genomic DNA sample. Prior to sequencing, the purified DNA was amplified by PCR with 338F and 806R primers for the hyper-variable V3-V4 region of the bacteria. Finally, the constructed amplicon libraries were sequenced on the Illumina MiSeq PE300 platform (Shanghai Personal Biotechnology Co., Ltd, Shanghai, China). Sequences processing was performed on the QIIME (Ver 1.9.1)-Ubuntu (Ver 14.04) platform followed previous study (Shu et al., 2015). All the raw data have been deposited into the NCBI SRA database under accession number SRP141657.

2.3. Quantitative real-time PCR for nitrogen functional genes

To explore the “key players” for the nitrogen removal under IC

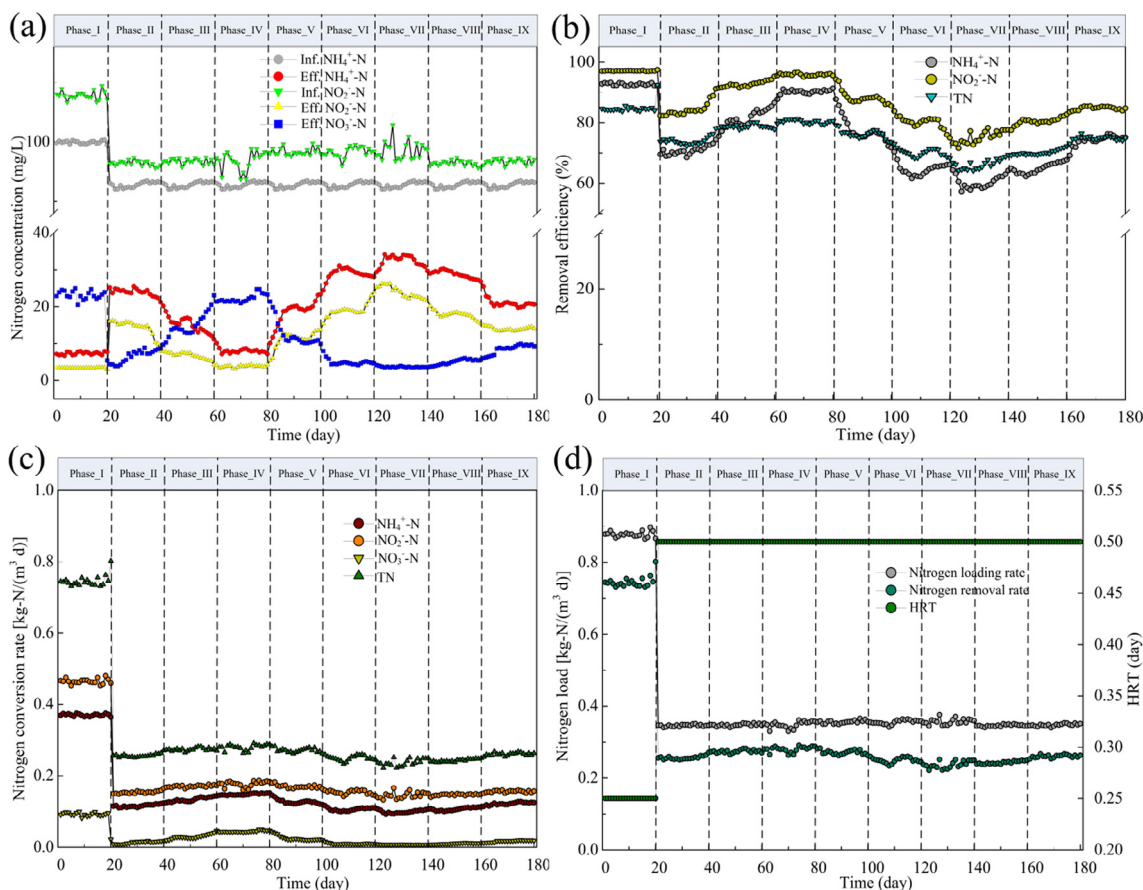


Fig. 1. The performance of nitrogen removal: (a) the profiles of influent and effluent $\text{NH}_4^+\text{-N}$, $\text{NO}_2^-\text{-N}$ and $\text{NO}_3^-\text{-N}$ concentrations; (b) the profiles of $\text{NH}_4^+\text{-N}$, $\text{NO}_2^-\text{-N}$ and TN removal efficiency; (c) the profiles of $\text{NH}_4^+\text{-N}$, $\text{NO}_2^-\text{-N}$, $\text{NO}_3^-\text{-N}$, and TN transformation rate; (d) the profiles of nitrogen loading rate (NLR), nitrogen removal rate (NRR) and HRT.

limitation, the absolute abundance of bacterial 16S rRNA, anammox 16S rRNA, AOB *amoA*, *nrfA*, *napA*, *narG*, *nirS*, *nirK*, and *nosZ* genes for each DNA samples was quantified by Mastercycler ep realplex (Eppendorf, Hamburg, Germany) based on the SYBR Green II method. The qPCR primers and protocols followed the previous study (Shu et al., 2015). In general, the qPCR mixtures (10 μL each) were prepared by mixing 5 μL SYBR® Premix Ex Taq™ II (Takara, Japan), 0.25 μL of each primer, 1 μL of genomic DNA and 3.5 μL dd H_2O . Each DNA sample was processed in triplicate to ensure reproducibility.

2.4. Chemical and statistical analyses

The influent and effluent water characteristics were monitored on a daily basis by chemical analyses. Prior to the analysis, each water sample was filtered through a 0.45 μm pore diameter membrane. The concentrations of $\text{NH}_4^+\text{-N}$, $\text{NO}_2^-\text{-N}$, $\text{NO}_3^-\text{-N}$, and TN were determined using a Lachat Quik Chem 8500 Flow Injection Analyzer (Lachat Instruments, Milwaukee, USA). The concentration of IC was measured daily using TOC analyzer (vario TOC cube, Elementar, Germany).

For statistical analyses, *P*-values were adjusted for multiple testing using a false discovery rate (FDR) of 5% with the *q*-value function implemented in *BiocLite R* (<https://bioconductor.org/biocLite.R>). *P* < 0.05 was considered significant for all statistical tests unless indicated otherwise. To minimize sequencing errors, OTUs (operational taxonomic units) present in the dataset as only singletons and doubletons were discarded. Then, remaining OTUs were defined as “abundant” when their average relative abundances were > 0.01% and “rare” when their abundances were < 0.005% across the entire dataset; those in between belong to transient sub-community (Wu et al., 2017).

Alpha diversity indices were calculated using QIIME platform on the base of cumulative sum scaling normalization (CSS) and sub-sampling. Principal coordinate analysis (PCoA) was applied to compare discrepancies among samples on the level of taxonomy and function using R with *vegan* packages based on the unweighted UniFrac distance matrices.

For network analysis, all possible pairwise Spearman’s rank correlations were calculated using *Hmisc* and *igraph* packages in R to investigate co-occurrence patterns of OTUs that were associated with abundant and rare sub-communities. Those correlations were considered statistically robust if the Spearman’s correlation coefficients (ρ) > 0.8 and *q* values < 0.01. Then, the co-occurrence networks visualization and modular analysis were performed using the Gephi platform (Ver 0.9.2, <https://gephi.org>). Moreover, global network-level and node-level properties were calculated to explore the topological properties of abundant and rare sub-networks according to previous studies (Ju et al., 2014; Ma et al., 2016). The R scripts for co-occurrence network analysis are found at <https://github.com/RichieJu520/Co-occurrence-network-analysis> (Ju et al., 2014).

Redundancy ordination analysis (RDA) was performed to determine the effects of operational parameters on the dominant genera and metabolic pathways of abundant and rare sub-communities. The related environmental variables were $\log(x + 1)$ transformed and then conducted using distance-based linear modeling (distLM) analysis with forward selection and an adjusted- R^2 selection procedure in PRIMER 7 (www.primers.com). To further explore significant associations between the operational parameters, dominant genera, and metabolic pathways of abundant and rare sub-communities, these Spearman’s rank correlation values were also examined using *corr.test* function

implemented in the *psych* R package.

To get a better understanding of functional genera and related metabolic pathways of abundant and rare sub-communities, the dataset of sequences for each OTU was blasted against the MIDAS database (<http://www.midasplatform.org>). Furthermore, the reconstruction of metabolic pathway and nitrogen functional genes was conducted via Tax4Fun (<http://tax4fun.gobics.de>) analysis based on the Silva SSU 128 database and KEGG category. Finally, the quantitative response associations between nitrogen transformation rates (i.e., $\text{NH}_4^+\text{-N}$, $\text{NO}_2^-\text{-N}$, and TN) and nitrogen functional gene fragments were performed using step regression models in R. All statistical analyses were conducted using R (Ver 3.4.1, R development core team 2014) with corresponding packages unless indicated otherwise.

3. Results and discussion

3.1. Nitrogen transformation of anammox granular system under IC constraints

The effect of IC on the nitrogen treatment performance of anammox granular systems is summarized in the Fig. 1. During phase I (0–20 days), the nitrogen loading rate (NLR) and nitrogen removal rate (NRR) were 0.88 and 0.74 kg-N/(m³·d), respectively. The average ratios of $\Delta\text{NO}_2^-/\Delta\text{NH}_4^+$ and $\Delta\text{NO}_3^-/\Delta\text{NH}_4^+$ were 1.26 ± 0.02 and 0.25 ± 0.04 , respectively. This result was accordant with the theoretical ratios for anammox given in the previous studies (Jin et al., 2014; Oshiki et al., 2016). Subsequently, other phases were established with distinct IC concentrations. During phase II (21–40 days), the experiment was performed without IC addition. As depicted in Fig. 1, the observed $\text{NH}_4^+\text{-N}$, $\text{NO}_2^-\text{-N}$, and TN removal efficiencies decreased to $70.83 \pm 1.50\%$, 84.43 ± 2.42 and $74.16 \pm 1.41\%$, respectively. The average ratio of $\Delta\text{NO}_2^-/\Delta\text{NH}_4^+$ increased to 1.33 ± 0.03 , but $\Delta\text{NO}_3^-/\Delta\text{NH}_4^+$ decreased to 0.11 ± 0.03 . In addition, the accumulation of $\text{NH}_4^+\text{-N}$ and $\text{NO}_2^-\text{-N}$ were observed in the effluent; the NLR and NRR sharply declined to 0.35 and 0.26 kg-N/(m³·d), respectively. These results revealed that insufficient IC had adverse effects on anammox activity (Zhang et al., 2018). One possible explanation is that surplus H^+ result in the anammox bacteria was inhibited by the free ammonia or free nitrous acid accumulation (Ma et al., 2017). During phases III and IV, with the increase of IC/TN ratios from 0 to 0.31, the observed $\text{NH}_4^+\text{-N}$, $\text{NO}_2^-\text{-N}$, and TN removal efficiencies increased gradually to $90.21 \pm 0.77\%$, $95.86 \pm 0.37\%$ and $80.41 \pm 0.60\%$, respectively. This result suggested that the anammox activity could be recovered by IC addition. Moreover, one-way ANOVA tests demonstrated that lower IC/TN ratios (0.06–0.31) had no significant influence ($P > 0.05$) on $\text{NH}_4^+\text{-N}$ and $\text{NO}_2^-\text{-N}$ removal. This may be because nitrogen transforming microorganisms are significantly resistant to lower IC/TN stresses.

During phases V, VI and VII, further increasing IC/TN from 0.62 to 1.24 declined the $\text{NH}_4^+\text{-N}$, $\text{NO}_2^-\text{-N}$, and TN removal efficiencies to $60.42 \pm 2.16\%$, $75.21 \pm 2.02\%$ and $66.36 \pm 1.62\%$. However, the calculated NLR and NRR only slightly decreased to 0.33 and 0.23 kg-N/(m³·d), respectively. These results indicated that although anammox activity was slightly suppressed by the IC/TN ratios (0.62–1.24), the nitrogen transforming microorganism had gradually adapted to the new conditions. During phases VIII and IX, the amount of IC increased to a IC/TN ratio of 1.87. As expected, the NLR and NRR in these phases was recovered, as revealed by the increased $\text{NH}_4^+\text{-N}$ ($74.30 \pm 1.65\%$) and $\text{NO}_2^-\text{-N}$ ($84.77 \pm 0.62\%$) removal efficiencies. One-Way ANOVA tests indicated that the nitrogen removal efficiencies showed significant differences under lower (0.06–1.24) and higher IC/TN ratio (1.56–1.87) stresses. Additionally, the accumulation of $\text{NH}_4^+\text{-N}$ and $\text{NO}_2^-\text{-N}$ in the effluent were alleviated under higher IC/TN ratios. These results were consistent with previous studies (Jin et al., 2014; Zhang et al., 2016), indicating that higher IC/TN ratios (1.56–1.87) could induce the effective recovery of anammox granular systems.

Throughout the whole experiment, above results revealed that influent IC/TN ratios had significant impacts on the anammox granular system. Under the relative lower IC/TN ratio (0.06–0.31) conditions, anammox bacteria were tolerant to lower IC stresses. Nevertheless, with the increase of IC (IC/TN ratio: 0.62–1.24), only a small fraction of surplus IC was utilized by anammox bacteria, resulting in an insufficient carbon resource for cellular growth. Therefore, the increased IC did not contribute to the improvement of nitrogen removal. In the last two phases (IC/TN ratio: 0.62–1.24), the NLR and NRR gradually recovered with sufficient IC addition. The possible reason for this phenomena is that when the high IC was supplied, some of the bicarbonate was consumed to neutralized the H^+ and surplus HCO_3^- was utilized by autotrophic and heterotrophic microorganisms to maintain their growth in the anammox system. Furthermore, it should be noted that the stoichiometric ratios of $\Delta\text{NO}_2^-/\Delta\text{NH}_4^+$ in phases VI–IX were higher than that in phase I, while the ratios of $\Delta\text{NO}_3^-/\Delta\text{NH}_4^+$ exhibited divergent results. The result indicated that nitrogen removal under higher IC supplementation was regulated by multiple nitrogen transforming pathways, such as denitrification ($\text{NO}_3^- \rightarrow \text{NO}_2^- \rightarrow \text{NO} \rightarrow \text{N}_2$) and dissimilatory nitrate reduction to ammonia (DNRA, $\text{NO}_3^- \rightarrow \text{NO}_2^- \rightarrow \text{NH}_4^+$) (Oshiki et al., 2016; Zhang et al., 2018).

3.2. Assemblage patterns and functional traits of abundant and rare sub-communities

After filtering and trimming, 145,882 high-quality reads were obtained from the nine phases (7799–23,931 reads per sample). To reduce any sequencing bias, the datasets were randomly sub-sampled at 7500 reads per sample and then clustered into an average of 2108 bacterial OTUs at 97% identity. For the whole community, the α -diversity indices in phase III, V and VIII were significantly different from the other phases ($P < 0.05$), indicating that IC/TN ratios had discrepant effects on the evenness and richness of bacterial community in above phases. Abundant, transient and rare taxa were comprise of 507, 264, and 1337 OTUs, accounting for 24.1%, 12.5%, and 63.4% of the total OTUs, respectively. In addition, there were 208 OTUs affiliated to core taxa, accounting for 9.8% of the total OTUs. Interestingly, OTUs affiliated with abundant and transient taxa dominated the core taxa, accounting for 43.3% (90 OTUs) and 56.7% (118 OTUs) of core taxa, respectively. None of rare taxa belonged to the core taxa, revealing that abundant and rare taxa exhibited contrasting community assemblage patterns in accordance with previous study (Wu et al., 2017).

In view of taxonomy level, the bacterial community structures of abundant and rare taxa differed substantially (Fig. 2a, b). *Proteobacteria* (30.6%), *Chloroflexi* (15.7%), *Bacteroidetes* (12.5%), *WWE3* (12.1%), and *Planctomycetes* (9.5%) were the dominant phyla in the abundant sub-community across the whole dataset. Compared with abundant sub-community, *Proteobacteria* (35.4%), *Actinobacteria* (17.9%), *Acidobacteria* (12.6%), *Chloroflexi* (12.4%), and *Bacteroidetes* (5.1%) largely dominated phyla in the rare sub-community. Results of the Wilcoxon rank sum tests indicated that assemblage patterns between abundant and rare sub-communities have remarkable differences ($P < 0.05$) under IC/TN ratio stresses. Similar to the previous study in a lab-scale anammox granular bioreactor (Lawson et al., 2017), results indicating that these phyla plays pivotal roles in the microbial interactions and metabolic activities of anammox granules.

Based on the functional potential and metabolic pathways of abundant and rare sub-communities, results showed that the top 21 metabolic pathways were shared by the above bacterial sub-communities. Amino acid utilization metabolism, transporters, nucleic acid metabolism, cellular response to stress and the nitrogen cycle were the predominant functional profiles across the whole dataset (Fig. 2c and d). However, the functional profiles related to amino acid utilization metabolism, cellular response to stress and nitrogen cycle were more prevalent in abundant sub-community than in rare sub-community. In contrast, functional traits affiliated with transporters and nucleic acid

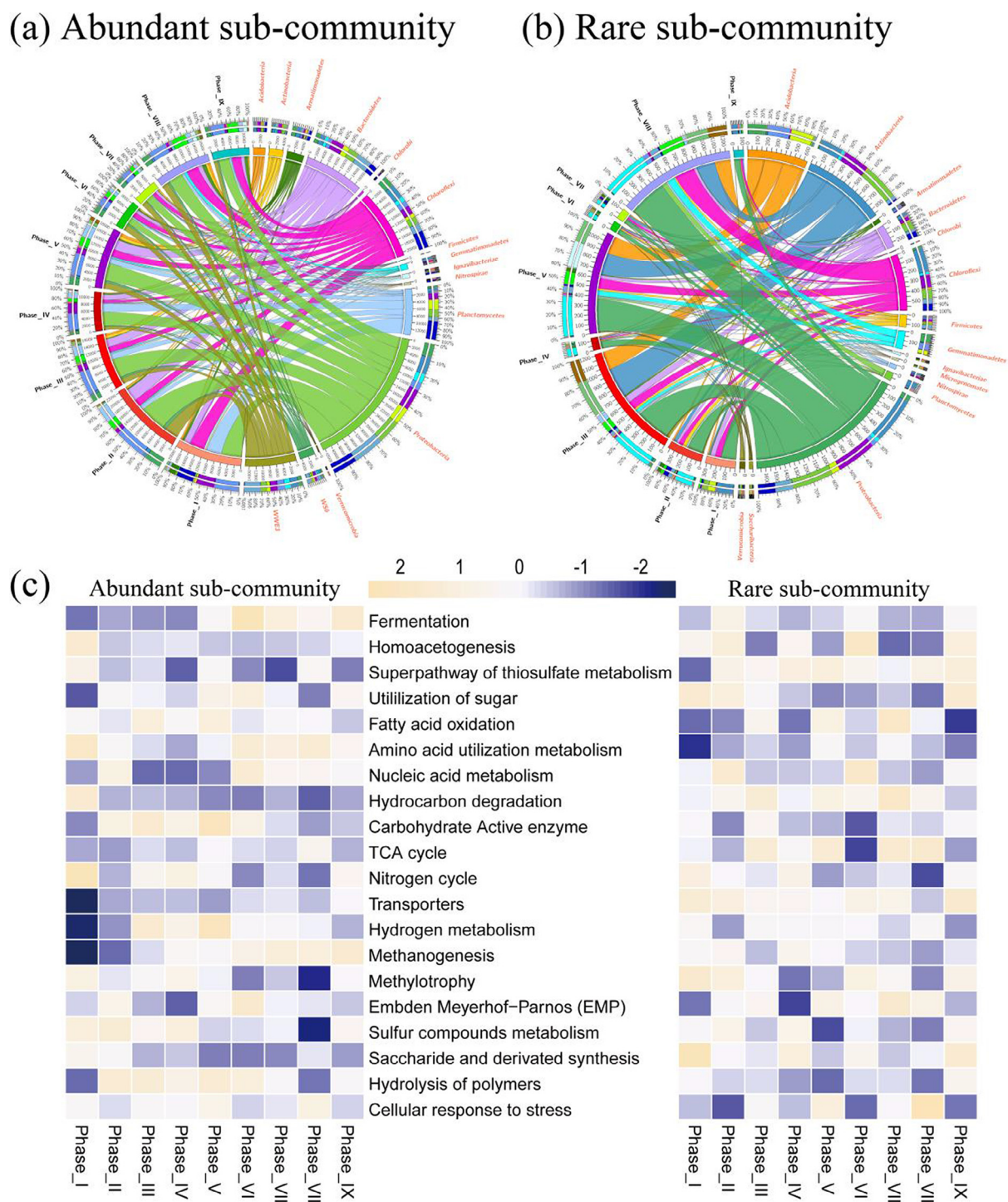


Fig. 2. Distribution of dominant phyla and functional traits in abundant and rare sub-communities in different treatment phases. The thickness of each ribbon represents the abundance of each taxon. The absolute tick above the inner segment and relative tick above the outer segment stand for the reads abundances and relative abundance of each taxon, respectively. Others refer to those unclassified reads. The data were visualized using Circos (Version 0.69, <http://circos.ca/>).

metabolism were more predominant in rare sub-community than those in abundant sub-community. Wilcoxon rank sum tests revealed that abundant and rare sub-communities had significant differences in the functional profiles ($P < 0.05$). Mantel statistic tests based on Spearman's rank correlation (999 permutations) further confirmed this result, indicating that abundant sub-communities were more similar to the whole community ($R^2 = 0.991$, $P < 0.001$) than rare sub-communities ($R^2 = 0.601$, $P = 0.02$). Furthermore, combined analysis of community assemblage and functional profiles on the basis of PCoA results revealed

clear distinct patterns of abundant and rare sub-communities. The first two PCoA components explained higher proportion of variance (53.4% on the taxonomy level and 81.8% on the function level) in abundant sub-community than that in rare sub-community (23.9% on the taxonomy level and 58.5% on the function level). These results suggested that the abundant and rare sub-communities had adopted distinct survival strategies under IC stresses (Liu et al., 2015). Moreover, the variance among phases appeared to be larger in the functional profiles than in the community structures, suggesting that functional traits dominate

the selection of bacterial communities under IC stresses (Yan et al., 2017).

To further explore the functional traits of these bacteria sub-community, vital functions related to energy and metabolism, such as the TCA cycle, nitrogen cycle, and amino acid metabolism were predominant in the abundant sub-community. These results suggested that abundant taxa contributed greatly to biomass and nutrient cycling (i.e., carbon and nitrogen cycling) and likely are responsible for the primary functions of the engineered ecosystem (Lawson et al., 2015; Saunders et al., 2016; Wu et al., 2017). In contrast, anammox process under IC constraints selected rare sub-community with specific functional profiles related to utilization of sugar, hydrogen metabolism, CAZy, nucleic acid metabolism, and EMP, indicating that rare taxa may be adapted to use specific substrates and metabolic products to maintain their cell growth and metabolic activity under IC stresses. Hence, the rare sub-community play a crucial role in anammox granular system response to perturbation and resilience (Ziegler et al., 2018).

3.3. The topological and taxonomic properties of the co-occurrence networks

To determine the co-occurrence patterns of different bacterial sub-communities, sub-networks for the community assemblage and functional traits were constructed. Based on the co-occurrence analysis for OTUs, 72,179 edges (Spearman's $|\rho| \geq 0.8$, $P < 0.01$) were captured between 1712 nodes for the global network. Of these nodes, 385 and 1296 nodes affiliated to abundant and rare sub-networks (Fig. 3a and b), respectively, reflecting that rare sub-communities had higher co-occurrence instances (edge/node ratio = 42.4) than that in abundant sub-communities (edge/node ratio = 33.8). Meanwhile, the topological features of sub-networks, as indicated by betweenness, closeness, node transitivity, and node degree, were discrepant between abundant and rare sub-communities (Fig. 3c–e). As shown in Fig. 3c, nodes in the abundant and transient sub-communities had higher betweenness centrality values, indicating a core location of abundant taxa in the whole network (Barberán et al., 2012). In contrast, low betweenness centrality values indicated that rare taxa had a peripheral distribution. In addition, it was observed that rare taxa had higher values of closeness, node transitivity, and degree than that in the abundant sub-community, suggesting higher intra-taxon associations of rare sub-community (Ju et al., 2014). However, the node-level topological features generally differed in the correlation network of metabolic pathway for the abundant and rare sub-communities. In the co-occurrence network on the base of functional traits, abundant sub-community exhibited higher co-occurrence instances (edge/node ratio = 5.2). Similar to the OTUs-based network, the abundant sub-community had a core location in the functional network. However, the abundant sub-community had higher values of closeness, eigenvector centrality, and degree than those in the OTUs-based network, indicating that abundant sub-community had high intra-taxon associations in the functional network. The functional profiles network thus presents contrasting co-occurrence patterns in comparison with OTUs-based network.

Moreover, topological features, including modularity (MD), clustering coefficient (CC), average path length (APL), graph density (GD), and network diameter (ND), were calculated to further confirm the co-occurrence patterns. For the OTUs- and function-based sub-networks, the values of MD, APL, and CC were higher than those in their corresponding Erdős-Rényi random networks, suggesting that these four sub-networks had modular structures and “small world” properties. Nevertheless, these topological features varied differently within each sub-networks. In the OTUs-based sub-networks, the high values of MD, CC, and AD confirmed a higher incidence of intra-associations in rare sub-communities. These results were consistent with previous study (Wu et al., 2017), demonstrating that abundant sub-community had wide niche breadths. Analogously, rare sub-communities present stronger inter-associations than abundant sub-communities, as revealed

by the values of MD, CC, and AD in the function-based networks.

Modularity analysis supported these findings. Results showed that the proportion of nine major modules in the OTUs- and function-based sub-networks differed substantially. It should be noted that metabolic pathways related to modules I and II accounted for a higher relative contribution to all modules than that modules affiliated with OTUs. Therefore, functional traits of abundant and rare sub-communities were clearly pivotal factors in governing modular structure in the co-occurrence networks. Additionally, amino acid utilization metabolism and nitrogen cycle accounted for modules I (23.5%) and II (16.9%), while nucleic acid metabolism and transporters were dominant in modules I (31.3%) and II (27.8%). This finding further highlighted the discrepancies ecological functional traits of abundant and rare sub-communities. Taken together, these results corroborated findings of community assemblage, suggesting that abundant and rare sub-community present divergent co-occurrence patterns. In particular, functional traits, and not taxonomic relatedness, play the predominant roles in determining the modular structure of abundant and rare sub-communities (Yan et al., 2017). This confirms the results of the PCoA analysis.

3.4. Driving force for abundant and rare microbial sub-communities

Given that environmental filtering and habitat heterogeneity greatly influences the diversity and ecological function of microbial communities (Barberán et al., 2012; Ju et al., 2014; Ortiz-Alvarez et al., 2018), the driving forces for community assemblage and functional traits of abundant and rare- sub-communities were further investigated. RDA and distLM analysis showed that effluent NO_3^- -N (adjust $R^2 = 62.58\%$, $P = 0.036$) was a key regulator in shaping the assemblage of abundant sub-community. In contrast, IC/TN (adjust $R^2 = 77.87\%$, $P = 0.026$) was the primarily driver in determining the assemblage of rare sub-community. Regarding the functional traits, results showed that IC/TN (adjust $R^2 = 47.11\%$, $P = 0.027$) was the strongest factor for functional profiles in the abundant sub-community, while effluent NH_4^+ -N (adjust $R^2 = 29.26\%$, $P = 0.001$) contributed greatly to metabolic pathways in the rare sub-community.

To further investigate the significant correlations of environment-species and environment-function, Spearman's correlation networks were constructed by calculating corresponding coefficients (Fig. 4). Generally, community assemblage and functional traits of bacterial sub-communities were constrained by different environmental attributes. For environment-species association networks, significant correlations between variables included effluent NO_3^- -N, NO_2^- -N and NH_4^+ -N and genera related to abundant sub-communities, followed by few significant associations between genera and other variables, such as IC/TN ratio and TN removal rate (Fig. 4a). Regarding the rare sub-communities, variables included NH_4^+ -N, NO_2^- -N and TN removal rate have more links connected to selected genera (Fig. 4b). For environment-function correlation networks, results revealed that functional profiles related to nitrogen removal were primarily connected to effluent NO_3^- -N, NH_4^+ -N, NO_2^- -N, and TN removal rate via positive correlations in both abundant and rare sub-community. However, results suggested that positive and negative associations between other functional traits and variables were generally distinct (Fig. 4c and d).

As mentioned above, these results indicate that abundant and rare sub-communities are governed by different operational parameters, which accords with previous studies in natural systems (Liu et al., 2015; Wu et al., 2017). Previous studies have been reported that *Ca. Brocadia sinica Candidatus Kuenenia* are R- and K-strategists respectively due to their different physiological characteristics. In the present study,

anammox bacteria such as *Ca. Brocadia sinica* and *Candidatus Jettenia*, which affiliated with the abundant sub-community, had positive correlation with effluent NO_3^- -N, NH_4^+ -N, NO_2^- -N, and TN removal rate, while had negative correlation with effluent effluent concentrations of NO_3^- -N and NH_4^+ -N. However, in the rare sub-community, *Candidatus Kuenenia* showed negative correlations with

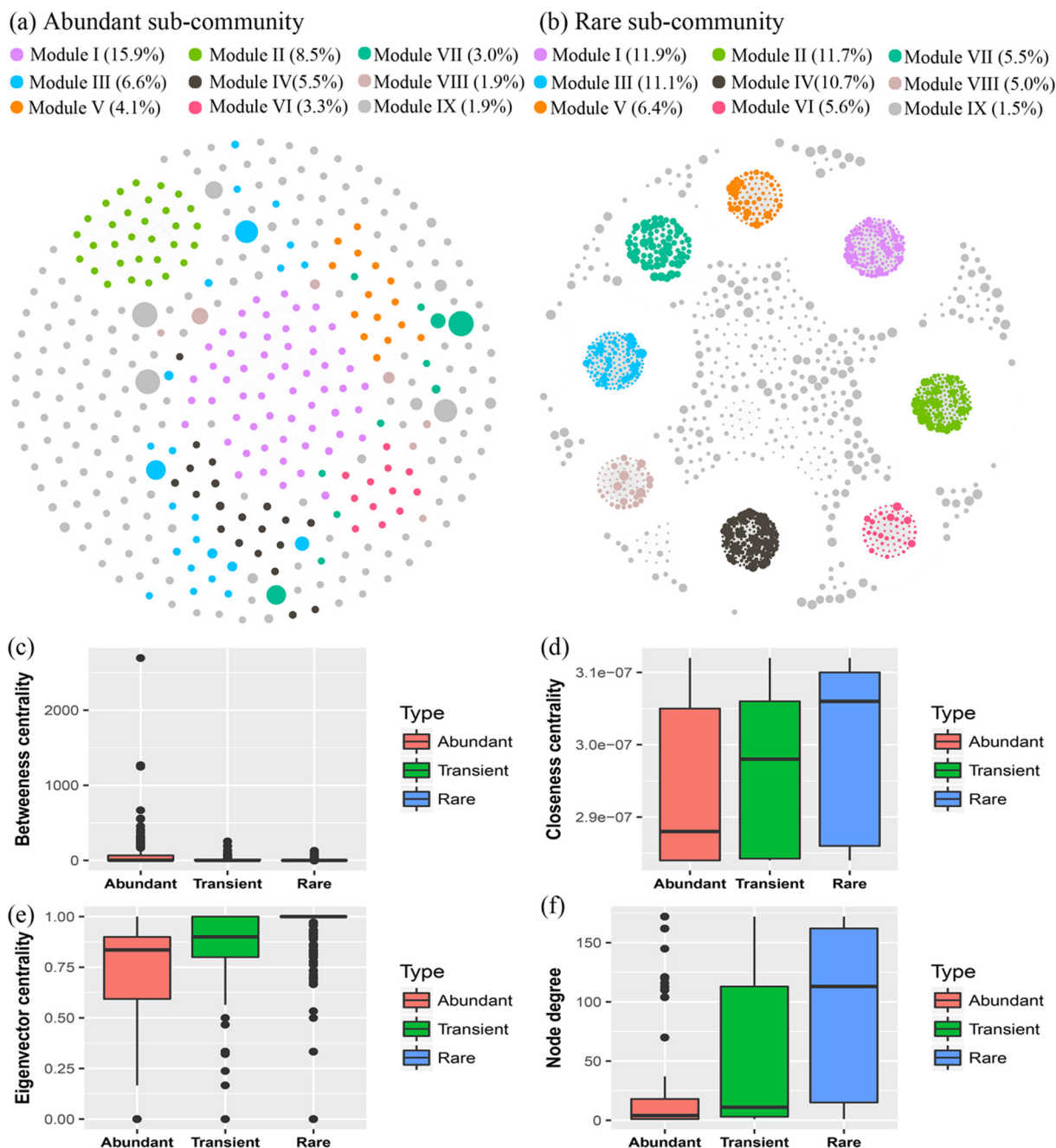


Fig. 3. The network analysis revealing the co-occurrence patterns among OTUs. The nodes were colored according to different sub-communities (a) and modularity class (b), respectively. A connection represents a strong (Spearman’s correlation coefficient $\rho > 0.8$ or $\rho < -0.8$) and significant ($q < 0.01$) correlation. The size of each node is proportional to the relative abundance of OTUs. The node-level topological features of different sub-communities, namely betweenness (c), closeness (d), transitivity (e), and degree (f). AT, MT, and RT represent abundant taxa, transient taxa, and rare taxa, respectively.

effluent NO_3^- -N, NH_4^+ -N and NO_2^- -N removal rate. The result indicated that “*Ca. Brocadia sinica*” and “*Ca. Kuenenia stuttgartiensis*” would compete for substrates under IC stresses due to their different kinetic and physiological characteristics. Additionally, “*Ca. Jettenia caeni*” had significantly differences with NO_2^- -N removal rate than “*Ca. Brocadia sinica*”, although both of two anammox bacteria were affiliated with abundant sub-community. Considering the nitrogen loading rate in the different phases, it was found that revealed that “*Ca. Brocadia sinica*” was able to outcompete “*Ca. Jettenia caeni*” at high loading rate but with lower IC stresses (< 0.62), whereas “*Ca. Jettenia caeni*” was able to proliferate at low nitrogen loading rate but with higher IC stresses (> 0.93). These result suggests that anammox bacteria present divergent survival patterns, which corroborated the results in the

previous study, suggesting that *Candidatus Brocadia* adopted the R-strategy to face the higher IC stresses, while *Candidatus Kuenenia* prefers the K-strategy to handle IC stresses (Kartal et al., 2013; Oshiki et al., 2016). Taken together, these results revealed that bacterial sub-communities have different ecological strategies under IC stresses; and anammox bacteria with similar metabolic function cannot coexist in the same environment due to their competitive exclusion and niche differentiation. These results are beneficial to explain or to predict how the system performance (e.g. NH_4^+ -N and NO_2^- -N removal) can respond to perturbation in operational conditions, considering a close linkages between microbial functional traits and process robustness. From an engineer’s perspective, realizing that (1) maintain rationally assembled microbial community assemblage patterns is pivotal to

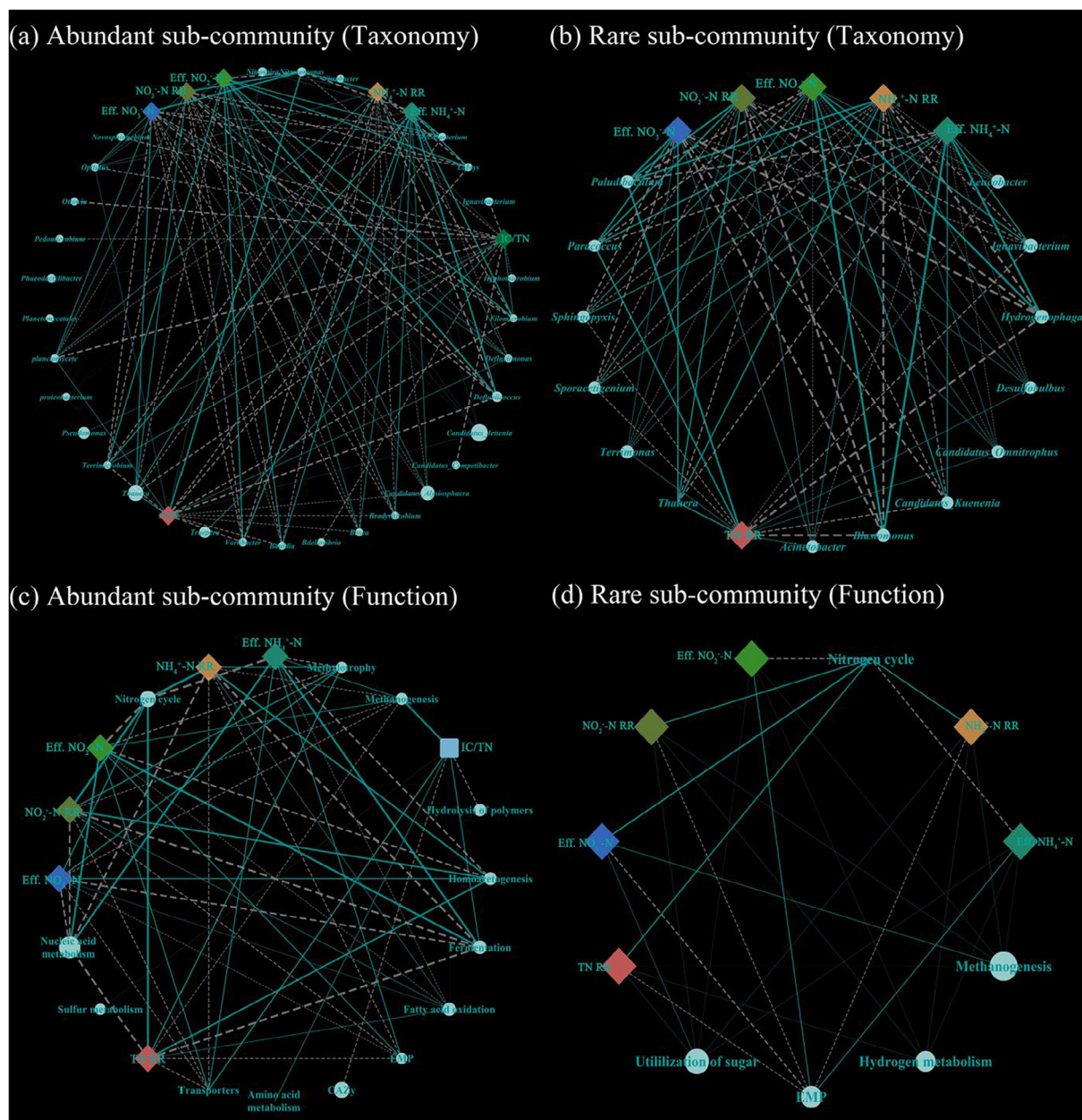


Fig. 4. Network analysis of the dominant genera, functional traits and environmental variables based on the correlation analysis. Only Spearman’s correlation coefficient $\rho > 0.6$ or $\rho < -0.6$ and significant ($q < 0.05$) correlations are shown. Each node represent the relative abundance of dominant genera or functional traits. Diamond-shaped nodes represent environmental variables. Solid line represent positive correlations and dash line represent negative correlations. The thickness of each line is proportional to the correlation coefficients of the connections.

sustaining long-term steady treatment performance and that (2) the bacteria assemblage patterns and functional traits is highly dependent on the microbial interactions, which can be manipulated indirectly via the control of certain key environmental variables (e.g. inorganic carbon concentrations) can change ways of thinking when it comes to operate anammox granular system.

3.5. Nitrogen metabolic pathways and adaptability of functional genera

To further quantitatively explore the ecological roles of abundant and rare sub-communities, we focused on the nitrogen metabolism to get a better understanding of functional gene fragments and nitrogen-transforming functional microorganisms in the anammox granular system. According to previous study, due to the *Hzs* and *Hdh* genes affiliated with anammox lack good representative sequences in the

KEGG database, but c-di-GMP represents the key second messenger for the aggregation of anammox under abiotic stresses. Therefore it was selected to investigate the anammox pathway. Abundance of c-di-GMP in phases IV, VII, and IX exceeded that in other phases. *nasA*, *nasB* and *nirA* genes related to assimilatory nitrate reduction were more prevalent in rare sub-community than those in abundant sub-community (Fig. 5c and e). For functional genes related to denitrification, *nosZ*, *qnorB* and *nirS* had higher predicted abundances in abundant sub-community than those in rare sub-community. For functional genes affiliated with dissimilatory nitrate reduction, *napA* and *nrfA* were predicted to be prevalent in the rare sub-communities (Fig. 5c and e). To sum up, these results indicated that nitrogen conversions, such as anammox, denitrification, nitrification and nitrogen fixation were mediated by abundant sub-communities, while assimilatory nitrate reduction and dissimilatory nitrate reduction to ammonium were

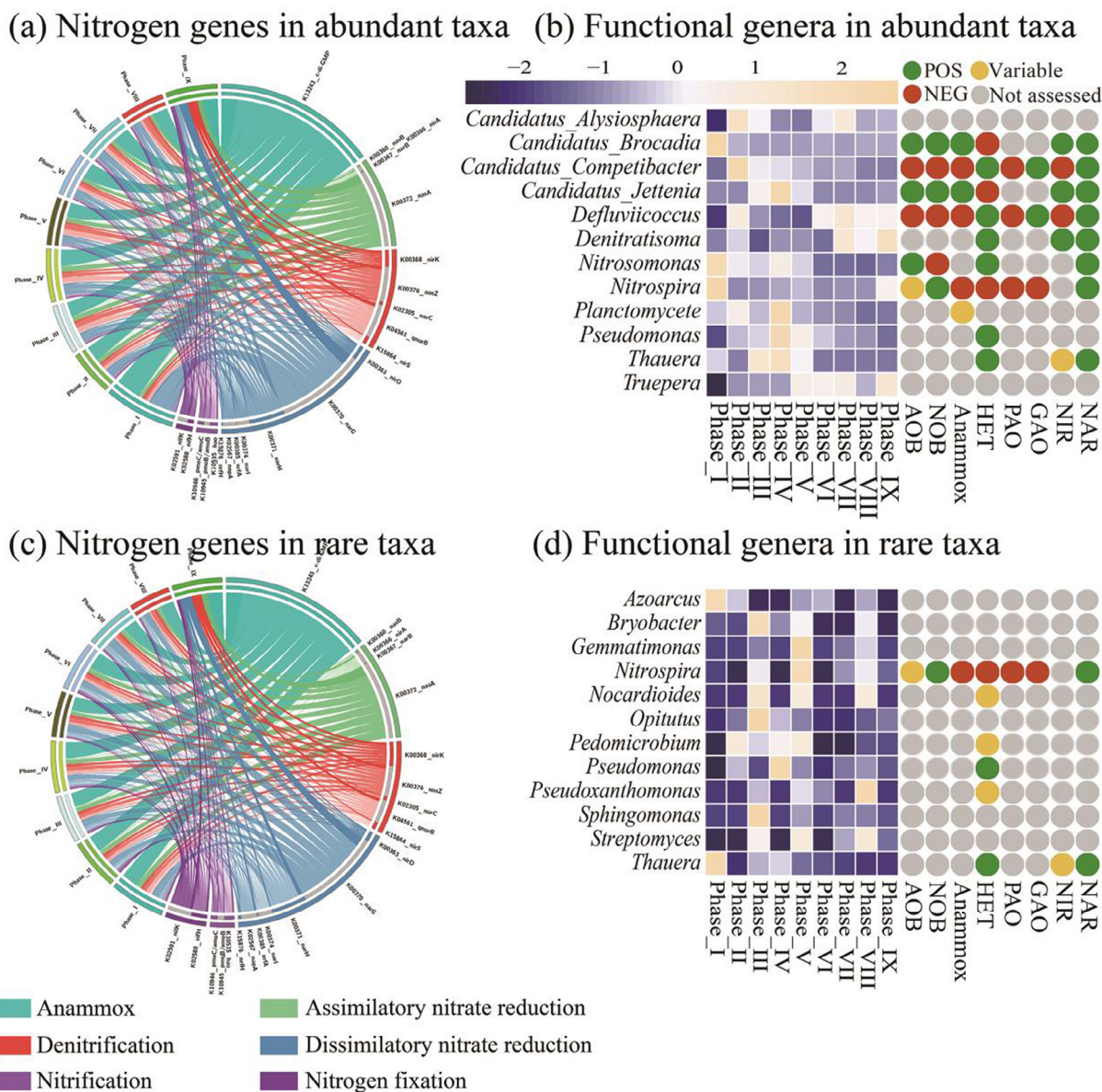


Fig. 5. The functional genes involved in microbial nitrogen cycling network as predicted by Tax4Fun based on KEGG category (a and c) and distribution of nitrogen-cycling-related functional genera in abundant and rare sub-communities according to MiDAS database (b and d). POS and NEG represent positive and negative associations, respectively.

regulated by rare sub-community.

Considering that process performance of anammox granular reactor was mediated by several functional species, an analysis of structure–function relationships was performed on the base of MiDAS database (Fig. 5b and d). Among all filtered genera, core functional genera (top 12 taxa with higher relative abundance) were annotated for abundant and rare sub-communities. Results from the MiDAS database showed that these functional species included 8 functional groups, namely ammonia oxidizing bacteria (AOB), nitrite oxidizing bacteria (NOB), anammox, heterotrophic microorganism (HET), phosphate accumulating organisms (PAO), glycogen accumulating organisms (GAO), nitrite-reduction bacteria (NIR), and nitrate-reduction bacteria (NAR). As shown in Fig. 5b, *Candidatus Brocadia* (0.22–15.74%) and *Candidatus Jettenia* (0.10–19.3) were prevalent anammox bacteria in the abundant sub-communities, while *Candidatus Kuenenia* (0–0.0013%) only appeared in the rare sub-communities. This result suggested that lower IC/TN ratios (< 0.31) were favorable for *Candidatus Brocadia*, while moderate IC/TN ratios (0.62–1.24) were beneficial to *Candidatus*

Jettenia. In particular, *Candidatus Kuenenia* was able to survive under higher IC/TN ratio stresses (1.56–1.87). Therefore, these anammox-related microorganisms have different ecological adaptabilities under IC stresses (Bhattacharjee et al., 2017; Kuypers et al., 2018; Oshiki et al., 2016). The *Nitrosomonas* (0.11–1.01%), which were reported as AOB, were only detected in the abundant sub-communities. This indicated that lower IC/TN ratio stresses was favorable for AOB growth. Interestingly, *Nitrospira* affiliated with NOB were shared by abundant and rare sub-communities. However, it was more abundant in the moderate and higher IC/TN ratios (> 0.62), suggesting that NOB may have adopted K-strategies to face the higher IC stresses (Kuypers et al., 2018). Functional species affiliated with HET, including *Pseudomonas* and *Thauera*, were shared by abundant and rare sub-communities. However, other denitrifiers such as *Candidatus Competibacter* and *Denitratisoma* only appeared in abundant sub-community. These denitrifiers can also perform NIR and NAR. Neither PAO nor GAO were annotated in the rare sub-community. Nevertheless, two kinds of GAO, *Candidatus Competibacter* and *Defluviicoccus* were found in abundant

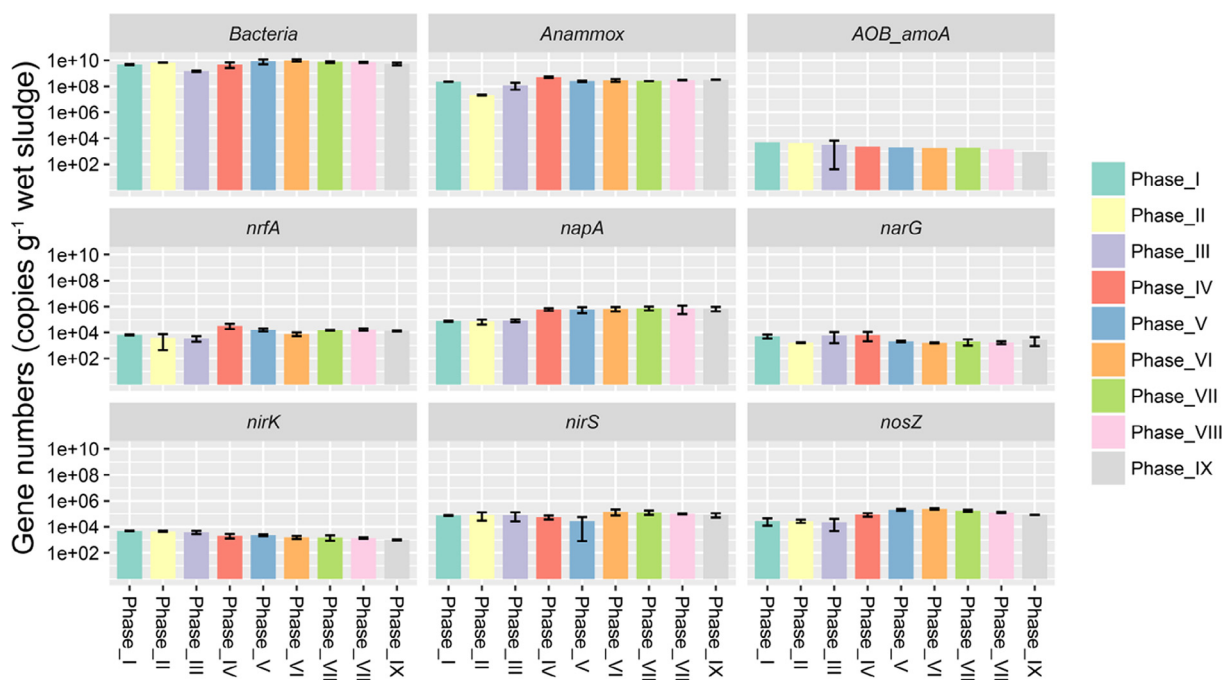


Fig. 6. Quantitative analysis of nitrogen functional genes in the different phases. Error bars represent standard deviation calculated from three independent experiments.

sub-communities under lower (< 0.62) and higher IC/TN (> 0.93) ratios, respectively. Taken together, lower IC/TN ratios (< 0.31) were beneficial to AOB and *Candidatus Brocadia*, moderate IC/TN ratios (0.62 – 1.24) were favorable for NOB, HET and *Candidatus Jettenia*; and *Candidatus Kueningenia* and GAO prefer to higher IC/TN ratio (1.56 – 1.87) situations. Obviously, environmental filtering (i.e., IC/TN ratios) are closely associated with ecological strategies of nitrogen transforming microorganisms (Ju et al., 2014; Kuypers et al., 2018).

To further corroborate the results of MiSeq sequencing, the functional genes associated with nitrogen conversions were quantified and quantitative response relationships were also performed (Fig. 6). The gene copies of anammox bacteria were nearly the same order of magnitude (1.26×10^8 – 5.85×10^8 copies/(g wet sludge)) except for phase II, confirming that anammox was the dominant microorganism in all phases and insufficient IC had adverse influences on anammox. The AOB gene copies in phases I–III were nearly one order of magnitude higher than that in phases IV–IX, which was consistent with Tax4Fun results that lower IC/TN ratios are favorable for nitrification. Similar results were observed in DNRA (i.e., *nrfA*, *napA*, *narG*) and denitrification groups (*nosZ*), confirming that nitrogen functional genera affiliated with these two pathways prefer to moderate and higher IC stress situations. The absolute abundance of *nirK* and *nirS* were not completely accordant with Tax4Fun results. The possible explanation is that anammox genomes affiliated with *Candidatus Jettenia* and *Candidatus Kueningenia* expressed *nirK* and *nirS* genes (Bhattacharjee et al., 2017). Based on qPCR, as revealed by stepwise regression models, the NH_4^+ -N transformation rate was jointly determined by *Anammox* (*narG* + *napA*) and (*nirS* + *nirK* + *nrfA*)/*Bacteria*, indicating that NH_4^+ -N consumption was mainly regulated by anammox bacteria and that NH_4^+ -N accumulation was mediated by the DNRA pathway. Given that the transformation of NO_2^- -N was collectively determined by *napA*/*Anammox*, *napA*/*AOB amoA*, and (*nirS* + *nirK* + *nrfA*)/*Bacteria*, suggesting that the anammox and denitrification are main pathways which responsible for NO_2^- -N consumption. However, NO_2^- -N accumulation was mediated by nitrification and DNRA, since NO_2^- -N was the intermediate substrate in these nitrogen conversions. For TN transformation rate, it was jointly controlled by *nirK*/*nrfA*, *napA*/*Anammox*, *napA*/*AOB amoA*, and (*nirS* + *nirK* + *nrfA*)/*Bacteria* (Wang et al.,

2016). Considering that abundant sub-community was responsible for anammox, denitrification and nitrification pathways, while rare sub-community responsible for DNRA pathway. It therefore concluded that abundant sub-community was the key regulator for NH_4^+ -N and NO_2^- -N consumption, while rare sub-community was responsible for NH_4^+ -N and NO_2^- -N accumulation. Collectively, these results indicated that nitrogen transformation pathways were mediated by different bacterial sub-communities. On the other hand, bacterial sub-communities adapted distinct survival strategies under different levels of IC constrains.

4. Conclusion

Results suggested that abundant and rare sub-communities exhibited divergent assemblage patterns and functional traits under IC/TN stresses, and that functional traits dominated the selection of bacterial sub-communities. Meanwhile, ecological strategies of bacterial sub-communities under IC stresses are closely associated with environmental variables. Additionally, lower IC/TN ratios (< 0.31) were beneficial to AOB and *Candidatus Brocadia*, moderate IC/TN ratios (0.62 – 1.24) were favorable for NOB, HET and *Candidatus Jettenia*; and *Candidatus Kueningenia* and GAO prefer to higher IC/TN ratio (1.56 – 1.87) situations. Finally, qPCR results corroborated that nitrogen transformation pathways were mediated by different bacterial sub-communities under different level of IC constrains.

Acknowledgements

This study was financially supported by National Science Foundation of China (41701291), China Postdoctoral Science Foundation (2017M620473), Ph. D start-up fund of Northwest A&F University (Z109021641), and Youth Elite Project of Northwest A&F University (Z109021805).

Appendix A. Supplementary data

Supplementary data associated with this article can be found, in the online version, at <https://doi.org/10.1016/j.biortech.2018.06.022>.

References

- Barberán, A., Bates, S.T., Casamayor, E.O., et al., 2012. Using network analysis to explore co-occurrence patterns in soil microbial communities. *ISME J.* 6 (2), 343–351.
- Bhattacharjee, A.S., Wu, S., Lawson, C.E., et al., 2017. Whole-community metagenomics in two different anammox configurations: process performance and community structure. *Environ. Sci. Technol.* 51 (8), 4317–4327.
- Daguerré Martini, S., Vanotti, M.B., Rodríguez Pastor, M., et al., 2018. Nitrogen recovery from wastewater using gas-permeable membranes: impact of inorganic carbon content and natural organic matter. *Water Res.* 137, 201–210.
- Hendriks, A.T.W.M., Langeveld, J.G., 2017. Rethinking wastewater treatment plant effluent standards: nutrient reduction or nutrient control? *Environ. Sci. Technol.* 51 (9), 4735–4737.
- Jia, X., Dini-Andreote, F., Falcao Salles, J., 2018. Community assembly processes of the microbial rare biosphere. *Trends Microbiol.* <http://dx.doi.org/10.1016/j.tim.2018.02.011>.
- Jin, R., Yu, J., Ma, C., et al., 2014. Transient and long-term effects of bicarbonate on the ANAMMOX process. *Appl. Microbiol. Biotechnol.* 98 (3), 1377–1388.
- Ju, F., Xia, Y., Guo, F., et al., 2014. Taxonomic relatedness shapes bacterial assembly in activated sludge of globally distributed wastewater treatment plants. *Environ. Microbiol.* 16 (8), 2421–2432.
- Kartal, B., Almeida, N.M., Maalcke, W.J., et al., 2013. How to make a living from anaerobic ammonium oxidation. *FEMS Microbiol. Rev.* 37 (3), 428–461.
- Kim, T.-S., Jeong, J.-Y., Wells, G.F., et al., 2013. General and rare bacterial taxa demonstrating different temporal dynamic patterns in an activated sludge bioreactor. *Appl. Microbiol. Biotechnol.* 97 (4), 1755–1765.
- Kimura, Y., Isaka, K., Kazama, F., 2011. Effects of inorganic carbon limitation on anaerobic ammonium oxidation (anammox) activity. *Bioresour. Technol.* 102 (6), 4390–4394.
- Kuypers, M.M., Marchant, H.K., Kartal, B., 2018. The microbial nitrogen-cycling network. *Nat. Rev. Microbiol.* <http://dx.doi.org/10.1038/nrmicro.2018.9>.
- Lackner, S., Gilbert, E.M., Vlaeminck, S.E., et al., 2014. Full-scale partial nitrification/anammox experiences—an application survey. *Water Res.* 55, 292–303.
- Lawson, C.E., Strachan, B.J., Hanson, N.W., et al., 2015. Rare taxa have potential to make metabolic contributions in enhanced biological phosphorus removal ecosystems. *Environ. Microbiol.* 17 (12), 4979–4993.
- Lawson, C.E., Wu, S., Bhattacharjee, A.S., et al., 2017. Metabolic network analysis reveals microbial community interactions in anammox granules. *Nat Commun.* 8.
- Lettinga, G., 2014. *My Anaerobic Sustainability Story*. LeAF Publisher, Wageningen.
- Liu, L., Yang, J., Zheng, Y., et al., 2015. The biogeography of abundant and rare bacterioplankton in the lakes and reservoirs of China. *ISME J.* 9 (9), 2068.
- Ma, B., Wang, H., Dsouza, M., et al., 2016. Geographic patterns of co-occurrence network topological features for soil microbiota at continental scale in eastern China. *ISME J.* 10 (8), 1891.
- Ma, H., Niu, Q., Zhang, Y., et al., 2017. Substrate inhibition and concentration control in an UASB-Anammox process. *Bioresour. Technol.* 238, 263–272.
- Ma, Y., Sundar, S., Park, H., et al., 2015. The effect of inorganic carbon on microbial interactions in a biofilm nitrification-anammox process. *Water Res.* 70, 246–254.
- Ortiz-Alvarez, R., Fierer, N., de Los Rios, A., et al., 2018. Consistent changes in the taxonomic structure and functional attributes of bacterial communities during primary succession. *ISME J.* <http://dx.doi.org/10.1038/s41396-018-0076-2>.
- Oshiki, M., Satoh, H., Okabe, S., 2016. Ecology and physiology of anaerobic ammonium oxidizing bacteria. *Environ. Microbiol.* 18 (9), 2784–2796.
- Saunders, A.M., Albertsen, M., Vollertsen, J., et al., 2016. The activated sludge ecosystem contains a core community of abundant organisms. *ISME J.* 10 (1), 11–20.
- Shade, A., Gilbert, J.A., 2015. Temporal patterns of rarity provide a more complete view of microbial diversity. *Trends Microbiol.* 23 (6), 335–340.
- Shu, D., He, Y., Yue, H., et al., 2015. Metagenomic insights into the effects of volatile fatty acids on microbial community structures and functional genes in organotrophic anammox process. *Bioresour. Technol.* 196, 621–633.
- Shu, D., Yue, H., He, Y., et al., 2018. Divergent assemblage patterns of abundant and rare microbial sub-communities in response to inorganic carbon stresses in a simultaneous anammox and denitrification (SAD) system. *Bioresour. Technol.* 257, 249–259.
- Wang, H., Ji, G., Bai, X., 2016. Distribution patterns of nitrogen micro-cycle functional genes and their quantitative coupling relationships with nitrogen transformation rates in a biotrickling filter. *Bioresour. Technol.* 209, 100–107.
- Wu, W., Logares, R., Huang, B., et al., 2017. Abundant and rare picoeukaryotic sub-communities present contrasting patterns in the epipelagic waters of marginal seas in the northwestern Pacific Ocean. *Environ. Microbiol.* 19 (1), 287–300.
- Yan, Y., Kuramae, E.E., de Hollander, M., et al., 2017. Functional traits dominate the diversity-related selection of bacterial communities in the rhizosphere. *ISME J.* 11 (1), 56.
- Yue, X., Yu, G., Liu, Z., et al., 2018. Start-up of the completely autotrophic nitrogen removal over nitrite process with a submerged aerated biological filter and the effect of inorganic carbon on nitrogen removal and microbial activity. *Bioresour. Technol.* 254, 347–352.
- Zhang, W., Wang, D., Jin, Y., 2018. Effects of inorganic carbon on the nitrous oxide emissions and microbial diversity of an anaerobic ammonia oxidation reactor. *Bioresour. Technol.* 250, 124–130.
- Zhang, X., Yu, B., Zhang, N., et al., 2016. Effect of inorganic carbon on nitrogen removal and microbial communities of CANON process in a membrane bioreactor. *Bioresour. Technol.* 202, 113–118.
- Ziegler, M., Eguiluz, V.M., Duarte, C.M., et al., 2018. Rare symbionts may contribute to the resilience of coral-algal assemblages. *ISME J.* 12 (1), 161–172.